

*Review Article (Invited)***Molecular dynamics simulations of amyloid- β peptides in heterogeneous environments**Yuhei Tachi^{1,2}, Satoru G. Itoh^{2,3,4}, Hisashi Okumura^{2,3,4}¹ Department of Physics, Graduate school of Science, Nagoya University, Nagoya, Aichi 464-8602, Japan² Institute for Molecular Science, National Institutes of Natural Sciences, Okazaki, Aichi 444-8787, Japan³ Exploratory Research Center on Life and Living Systems (ExCELLS), National Institutes of Natural Sciences, Okazaki, Aichi 444-8787, Japan⁴ Department of Structural Molecular Science, SOKENDAI (The Graduate University for Advanced Studies), Okazaki, Aichi 444-8787, Japan

Received October 18, 2021; Accepted March 31, 2022;

Released online in J-STAGE as advance publication April 2, 2022

Edited by Akio Kitao

Alzheimer's disease is thought to be caused by the aggregation of amyloid- β (A β) peptides. Their aggregation is accelerated at hydrophilic/hydrophobic interfaces such as the air–water interface and the surface of monosialotetrahexosylganglioside (GM1) clusters on neuronal cell membranes. In this review, we present recent studies of full-length A β (A β 40) peptides and A β (16–22) fragments in such heterogeneous environments by molecular dynamics (MD) simulations. These peptides have both hydrophilic and hydrophobic amino-acid residues and tend to exist at the hydrophilic/hydrophobic interface. Therefore, the peptide concentration increases at the interface, which is one of the factors that promote aggregation. Furthermore, it was found that A β 40 forms an α -helix structure and then a β -hairpin structure at the interface. The β -hairpin promotes the formation of oligomers with intermolecular β -sheets. It means that not only the high concentration of A β 40 at the interface but also the structure of A β 40 itself promotes aggregation. In addition, MD simulations of A β 40 on recently-developed GM1-glycan clusters showed that the HHQ (13–15) segment of A β 40 is important for the recognition of GM1-glycan clusters. It was also elucidated that A β 40 forms a helix structure in the C-terminal region on the GM1-glycan cluster. This result suggests that the helix formation, which is the first step in the conformational changes toward pathological aggregation, is initiated at the GM1-glycan moieties rather than at the lipid-ceramide moieties. These studies will enhance the physicochemical understanding of the structural changes of A β at the heterogeneous interfaces and the mechanism of Alzheimer's disease pathogenesis.

Key words: aggregation, β -sheet, α -helix, air–water interface, GM1 cluster**◀ Significance ▶**

The aggregates of amyloid- β (A β) peptides are considered the cause of Alzheimer's disease. A β aggregation is accelerated at hydrophilic/hydrophobic interfaces such as the air–water interface and the neuronal cell membrane surface. Therefore, understanding the mechanism of the A β aggregation in such heterogeneous environments is significant for developing therapeutic agents and preventive drugs. In this review, we survey several studies that have elucidated the mechanism of the A β aggregation at the interfaces at the atomic level by molecular dynamics simulations.

Introduction

Proteins are normally folded correctly and maintain their functions in the body. However, at high concentrations, many proteins aggregate to form oligomers, spherical aggregates, or amyloid fibrils, needle-like aggregates. These protein aggregates are associated with about 40 human neurodegenerative diseases [1-5]. For example, Alzheimer's disease is associated with amyloid- β (A β) peptides, Huntington's disease with polyglutamine tracts, and Parkinson's disease with α -synuclein.

A β is an intrinsically disordered protein with 40–43 amino-acid residues. It usually consists of 40 or 42 residues. A β with 40 residues is known as A β 40, and that with 42 residues is known as A β 42. A β and its fragments have been the subject of many experimental and computational studies [5-18]. For example, solid-state nuclear magnetic resonance (NMR) experiments have revealed that two intermolecular β -sheet structures are formed in A β 40 amyloid fibrils [8]. In this model, the two intermolecular β -sheets consist of residues 10–22, referred to as β 1, and residues 30–40, referred to as β 2. The majority of the β 1 and β 2 regions are composed of hydrophobic residues. Structural models of A β fibrils with different β -sheet regions have also been reported [11,13,14].

Deposition of A β peptides is observed in the brains of Alzheimer's disease patients [19,20], and A β oligomers and amyloid fibrils show toxicity to neurons [21-24]. To develop therapeutic and preventive agents for Alzheimer's disease, it is important to understand the aggregation process of A β at the atomic level. However, the mechanisms by which oligomers and amyloid fibrils are formed are still not fully understood.

Several experiments have reported that the aggregation of A β peptides is promoted at hydrophilic/hydrophobic interfaces such as the air–water interface (Fig. 1a) [25-27] and the surface of monosialotetrahexosylganglioside (GM1) clusters on neuronal cell membranes (Fig. 1b) [28-30]. Gangliosides are amphiphilic substances that contain glycans as hydrophilic groups, lipids as hydrophobic groups, and one or more sialic acids in the glycan region, as shown in Fig. 2. The ganglioside that is thought to promote the A β aggregation is GM1 [30]. In fact, A β -bound GM1 has been found in the brains of Alzheimer's disease patients [31].

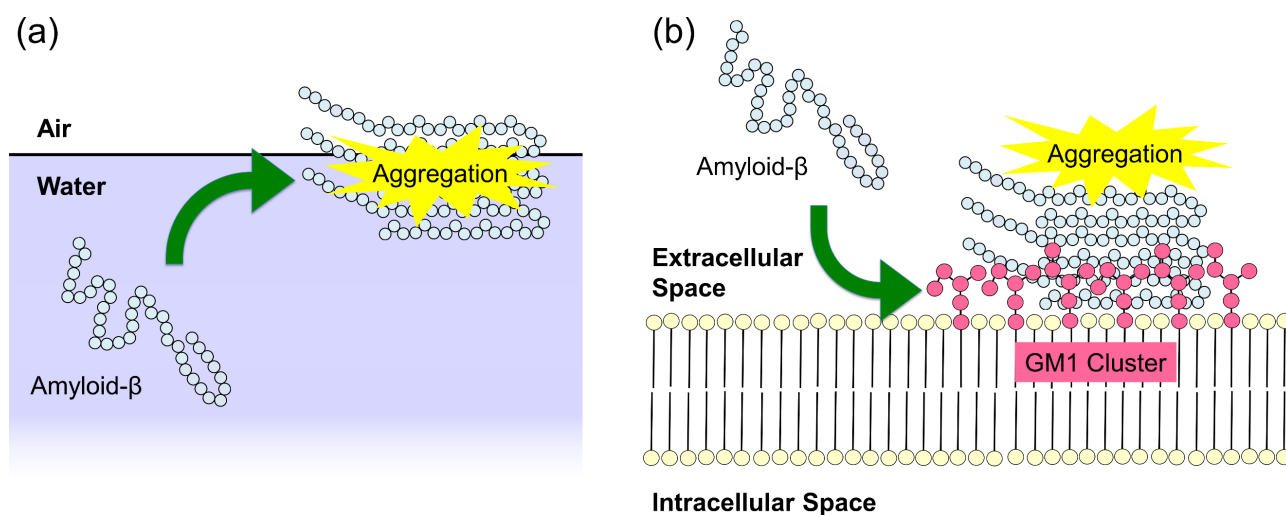


Figure 1 Schematic illustration of aggregation of A β peptides at (a) the air–water interface and (b) the GM1-cluster surface.

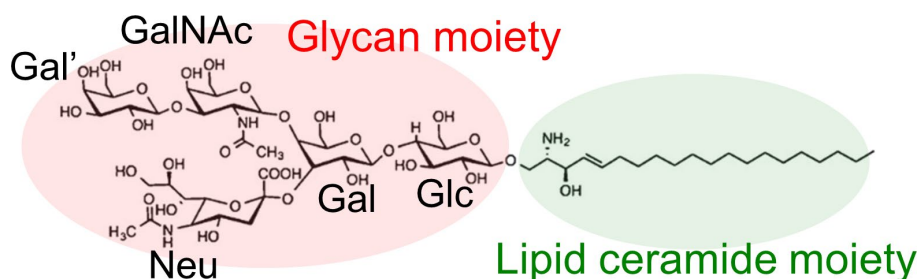


Figure 2 Glycan and lipid ceramide moieties of GM1. Reproduced with permission from Ref. [32].

In order to understand why A β peptides tend to aggregate at these interfaces, the aggregation of A β peptides in such heterogeneous environments has attracted attention both experimentally [28] and theoretically [27,33,34]. The atomic-level structural changes during the A β aggregation process can be revealed by molecular dynamics (MD) simulations. Many MD simulations of A β and related peptides have been performed [15-18], such as the monomeric state [27,34-43], dimerization [44-57], oligomerization [33,58-66], amyloid-fibril elongation [67-79], amyloid-fibril stability [80-86], aggregation inhibition [87,88], and dissociation process [89-92]. However, most of the computational studies of A β have been performed in bulk water, and relatively few MD simulations have focused on the effect of heterogeneous environments such as hydrophilic/hydrophobic interfaces. In this review, we explain the MD simulations of A β peptides in heterogeneous environments that we have performed so far. This review article is an extended version of the Japanese article [32].

First, we describe MD simulations in which aggregation of 100 peptides at the air–water interface was observed [33]. However, it is difficult to perform aggregation simulations with full-length A β peptides in explicit water. In this study, A β fragments consisting of 7 amino-acid residues, A β (16–22), were used. The A β (16–22) peptides are also known to form amyloid fibrils by experiments [93], and it is relatively easy to reproduce the formation of intermolecular β -sheets in MD simulations [60,94-96]. All-atom MD simulations of 100 A β (16–22) peptides were performed in explicit water with an air–water interface to observe the aggregation process. The simulations of this system revealed the aggregation mechanism of a large number of peptides at the interface [33].

Next, we introduce MD simulations of a single A β 40 peptide at the air–water interface to reveal the structure of a full-length A β peptide in a heterogeneous environment [27]. To understand the effect of the interface, it is essential to clarify the difference between an A β peptide at the air–water interface and that in bulk water. We therefore also compare A β 40 with and without an interface (i.e., bulk water).

Finally, we describe MD simulations of A β 40 on the surface of GM1-glycan clusters as a heterogeneous environment that is more similar to the neuronal membrane surface [32,34]. Recently, GM1-glycan clusters, in which GM1 glycans are transplanted on supramolecular metal complexes, have been developed [97]. Several experimental [97] and computational [34,98] studies have been performed using this GM1-glycan cluster as a model system to elucidate the binding process of A β to the GM1 cluster. As the last topic of this review, the structural change of A β upon binding to the GM1-glycan cluster is discussed.

Aggregation of A β (16–22) Peptides at Air–Water Interfaces

In this section, we present MD simulations of A β (16–22) peptides at the air–water interfaces [33]. An A β (16–22) peptide consists of the 16th to 22nd amino-acid residues of an A β peptide. It is a seven-residue peptide with the amino-acid sequence KLVFFAE, which corresponds to a part of the β 1 region of the A β peptide. The A β (16–22) peptides form oligomers and amyloid fibrils by themselves. It is one of the most studied peptides by MD simulations because it is shorter and aggregates more easily than the full-length A β peptides, A β 40 and A β 42.

Molecular dynamics simulations were performed as follows. First, 200 fully-extended A β (16–22) peptides with all dihedral angles φ and ψ of 180°, were randomly distributed with 325,000 water molecules in a cubic simulation box with a side length of 217.51 Å. The total number of atoms of this system is 1,000,000. Five different initial conditions were prepared using different random numbers. Both coordinates and the momentum were different from each other. As equilibration runs, MD simulations in the isothermal–isobaric ensemble were performed for 10 ps at 310 K and 0.1 MPa using the Nosé–Hoover thermostat [99-101] and the Andersen barostat [102]. Although the volume was equilibrated during these short MD simulations, the A β (16–22) peptides did not start to aggregate yet. Then, the A β (16–22) peptides and water molecules in the upper and lower quarters of the z-axis were removed so that 100 A β (16–22) peptides and 162,500 water molecules remained, as shown in Fig. 3(a). The total number of atoms was 500,000. The final simulation-box sizes obtained from these equilibration MD simulations were slightly different in the order of 0.1 Å. However, the box size in the following long simulations was unified and fixed at 217.69 Å, which is the average of the final simulation box sizes. We then performed a canonical MD simulation for 300 ns from each initial condition at 310 K using the Nosé–Hoover thermostat [99-101]. The MD simulations were performed using the Generalized-Ensemble Molecular Biophysics (GEMB) program developed by one of the authors (H. O.). This program has been used to simulate several proteins and peptides [103-118]. Using this program, we can perform MD simulations with the generalized-ensemble algorithms [119-123], such as replica-exchange [124,125], replica-permutation [39,126], multicanonical [127-130], and multibaric-multithermal [131-134] algorithms. However, usual canonical MD simulations [99-101] were performed in this study. As shown in Fig. 3(a), even though the top and bottom quarters of the simulation box are initially in a vacuum, all A β (16–22) peptides and most water molecules did not evaporate because the temperature was not so high. Therefore, this interface was naturally maintained without any additional force. The upper and lower quarters of the simulation box were actually vacuum or water vapor, although they are referred to as air here. For other details of the simulation conditions, please refer to Ref. [33].

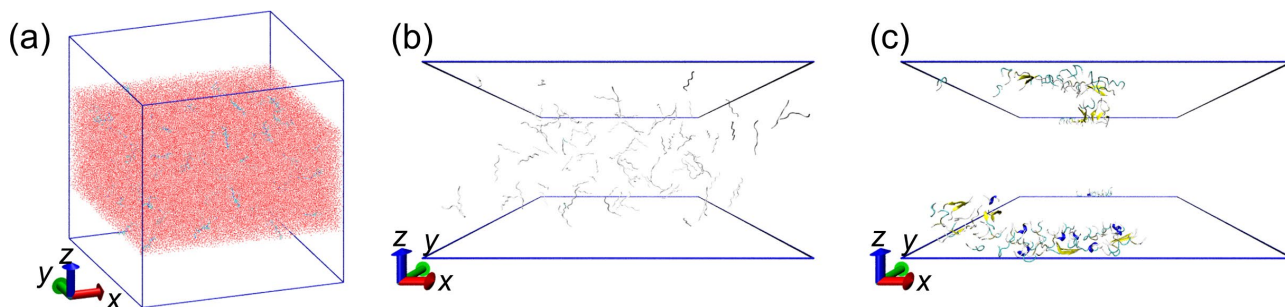


Figure 3 (a) Initial structure of A β (16–22) solution with the air–water interface. (b) Side view of the initial conformations of A β (16–22) peptides. (c) Side view of the final conformations of A β (16–22) peptides. Water molecules are not shown in panels (b) and (c). The blue frames in panels (b) and (c) indicate the air–water interface. Reproduced with permission from Ref. [33].

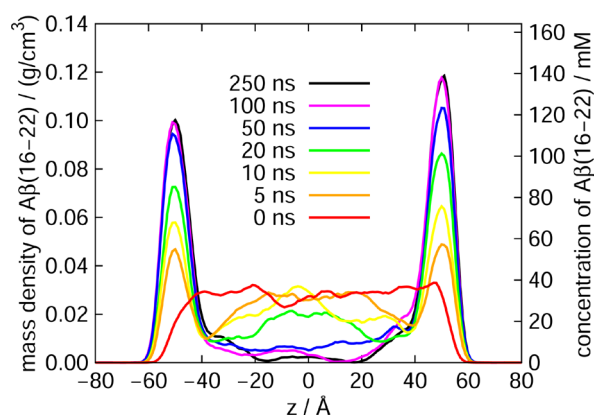


Figure 4 Mass density distribution along the z -axis of A β (16–22) atoms. The vertical axis is also shown as the concentration of the A β (16–22) peptides. Reproduced with permission from Ref. [33].

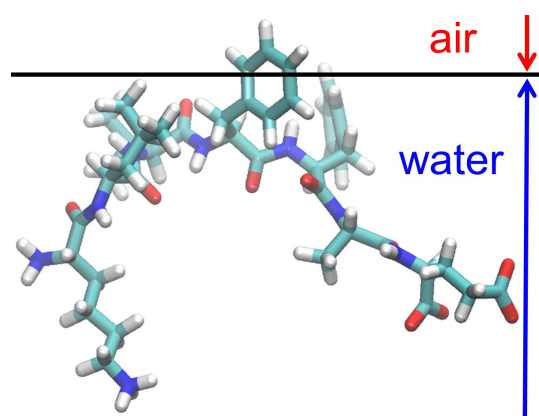


Figure 5 A typical snapshot of A β (16–22) at the air–water interface. Reproduced with permission from Ref. [33].

It was observed that the A β (16–22) peptides gradually moved to the air–water interface with time in all MD simulations from the five initial conditions. In the end, all A β (16–22) peptides moved to the interface, as shown in Fig. 3(c). Figure 4 shows the mass-density distribution of the A β (16–22) atoms along the z -axis and the concentration of the A β (16–22) peptides. The A β (16–22) peptides were almost uniformly distributed from $z = -40$ Å to $z = +40$ Å at the beginning of the MD simulation. As these molecules gradually moved to the air–water interface, the density of the A β (16–22) peptides increased at the interface and decreased in bulk. This is because A β (16–22) has both hydrophilic (Lys, Glu) and hydrophobic (Leu, Val, Phe, Ala) residues, and the hydrophilic residues tend to exist in water, while the hydrophobic residues tend to exist in the hydrophobic region, air, as shown in Fig. 5. These results can also be applied to the full-length A β peptides. That is, the reason why the full-length A β peptides exist mainly on the surface of neurons is also that this surface is the hydrophilic/hydrophobic interface and the A β peptides have both hydrophilic and hydrophobic residues. In other words, the A β peptide is an amphiphilic molecule like a surfactant. Therefore, the concentration of the A β peptides at the interface increases, and they tend to aggregate there.

A β 40 Peptide at the Air–Water Interface

In this section, we explain the structure of the full-length A β peptide, A β 40, at the air–water interface [27]. The amino-acid sequence of A β 40 is DAEFRHDSGYEVHHQKLVFFAEDVGSNKGAIIGLMVGGVVV. The N- and C-termini are uncapped. MD simulations of an A β 40 peptide were performed in a system with air–water interfaces. The air–water interface was again prepared by removing half the water molecules in a cubic simulation box with the side length of 108.0 Å. Nine different initial conditions (three coordinates \times three velocities) were employed for statistical analysis. The initial

structure of A β 40 was fully-extended with all dihedral angles φ and ψ of 180° for all the three initial coordinates. An MD simulation was performed from each initial condition for 230 ns after an equilibration run for 10 ns. Temperature was controlled at 350 K by the Nosé-Hoover thermostat [99-101]. In the A β (16–22) system in the previous section, the temperature was set at 310 K. The reason for setting the temperature at 350 K here is to make it easier to obtain various conformations of A β 40 because it is longer than A β (16–22). For comparison, MD simulations of the A β 40 peptide in bulk water were also performed. The initial structure of A β 40 in bulk water was also the fully-extended structure. Nine different initial conditions were prepared as well, with nine different initial velocities. The side length of the cubic unit cell was 91.1 Å. An MD simulation was performed from each initial condition for 230 ns after an equilibration run for 10 ns, again. For other simulation details, please refer to Ref. [27].

A β 40, like A β (16–22) peptide, was observed to exist at the air–water interface. To investigate the structure of A β 40 at the interface, the average distance from the interface to the C $_{\alpha}$ atom of each residue was calculated, as shown in Fig. 6(a). The positive value of this distance means that the C $_{\alpha}$ atom exists in the water, and the negative value means that it exists in the air. We can see that A β 40 has an up-and-down shape at the interface. The up-and-down shape was observed in all MD simulations starting from the nine initial conditions. Our simulations, therefore, can be regarded as sufficiently sampling the conformational space. This result is in good agreement with the NMR experiments for the structure of A β 40 on lyso-GM1 micelles [135], in which Val12–Gly25, Ile31–Val36, and Val39–Val40 of A β 40 (red lines in Fig. 6(a)) were found to bind to lyso-GM1 micelles. Note that Val12–Gly25 almost coincides with the β 1 region, and Ile31–Val36 and Val39–Val40 are included in the β 2 region. We remark that the structure of A β 40 at the air–water interface has not yet been revealed experimentally. Here, we showed that the MD simulation results of A β 40 at the air–water interface are consistent with the experimental results on lyso-GM1 micelles. In addition, these results agree with the experimental results on GM1 micelles, too [136]. Therefore, we can think that the result that A β 40 takes the up-and-down shape may hold for other hydrophilic/hydrophobic interfaces in general.

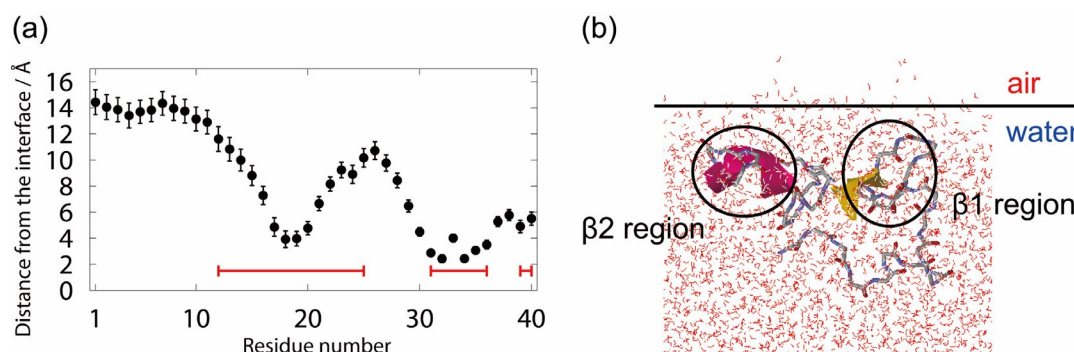


Figure 6 (a) The average distance from the C $_{\alpha}$ atom of each amino-acid residue of A β to the interface. The red lines indicate the residues bound to the lyso-GM1 micelle in the experiment [135]. (b) A typical snapshot of A β 40 at the interface. Reproduced with permission from Ref. [27].

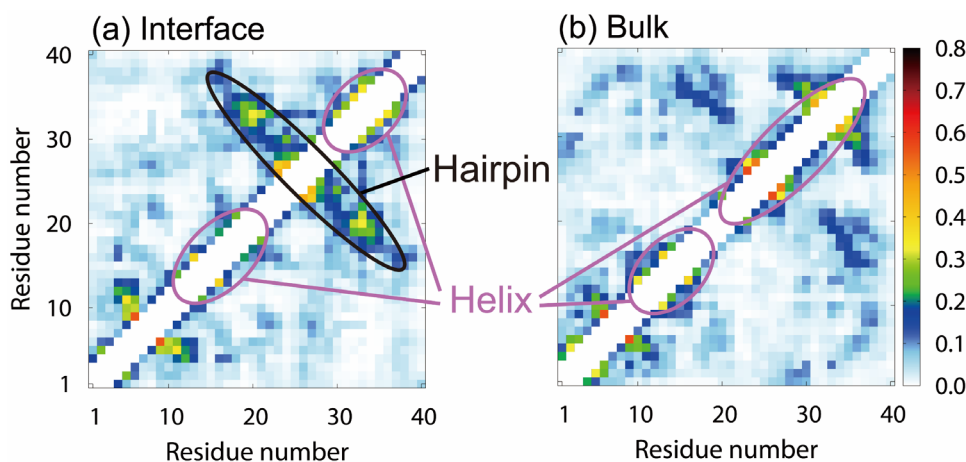


Figure 7 Contact probabilities of C $_{\alpha}$ atoms (a) at the air–water interface and (b) in bulk water. Reproduced with permission from Ref. [27].

Figure 6(b) shows a typical structure at the interface obtained from the simulations. The $\beta 1$ and $\beta 2$ regions are bound at the interface, and the N-terminal region and the linker region between $\beta 1$ and $\beta 2$ are in the aqueous solution. Like the A β (16–22) peptide, A β 40 can be regarded as an amphiphilic molecule and tends to exist at a hydrophilic/hydrophobic interface.

Although the pH condition at the air–water interface has been discussed, it is still controversial whether the interface is acidic or basic [137–139]. In our simulation study, the pH of the interface was considered to be the same as that in bulk. However, since it is the hydrophobic residues that are exposed to the air at the interface, the effect of pH on the up-and-down shape obtained in the MD simulations is considered to be small. Tahara and coworkers have measured the state of cytochrome c at the air–water interface using electronic sum frequency generation spectroscopy [140]. Their results show that the hydrophobic residues are exposed and denatured in the air at the interface. They also concluded that the effect of pH on the interfacial denaturation of cytochrome c was small because the effect of the interfacial perturbation was predominant.

To investigate the effect of the air–water interface on the structure of A β 40, the contact probabilities of C_{α} atoms were also calculated from the MD simulations. Figures 7(a) and 7(b) show the contact probabilities for the system with the interface and in bulk water, respectively. The $\beta 1$ and $\beta 2$ regions form helix structures at the interface, which is consistent with the experimental results on the lyso-GM1 micelles [135]. In addition, a β -hairpin structure is formed when the $\beta 1$ and $\beta 2$ regions have contact with each other. On the other hand, in bulk water, as shown in Fig. 7(b), both the $\beta 1$ and $\beta 2$ regions have helix structures, but the β -hairpin structure is hardly formed. The difference between the β -hairpin formation probability at the interface and that in bulk water leads to a difference in the oligomer formation ability. It was reported by the MD simulations of several A β fragments that the β -hairpin structure promotes the formation of intermolecular β -sheet structures with other A β fragments [48,62]. The importance of the β -hairpin structure in the formation of oligomers with intermolecular β -sheet structures has also been shown in experimental studies [141,142]. As we explained in the previous section, since A β 40 has both hydrophilic and hydrophobic residues, the A β 40 concentration increases at the hydrophilic/hydrophobic interface, and the aggregation is enhanced there. However, it is not only the high concentration of A β 40 but also the structure of A β 40 itself that promotes the aggregation.

Next, we explain why the β -hairpin structure is stabilized at the interface. As shown in Fig. 6, the $\beta 1$ and $\beta 2$ regions tend to be trapped at the interface, and these regions only move at the interface. Therefore, the motion of the $\beta 1$ and $\beta 2$ regions is restricted to two dimensions (Fig. 8). In bulk water, on the other hand, the $\beta 1$ and $\beta 2$ regions can move in three dimensions. Entropy increases as they take different conformations in bulk water. However, at the interface, the entropy increase is suppressed due to the two-dimensional motion. To reduce the enthalpy under this restriction, hydrogen bonds are formed between the $\beta 1$ and $\beta 2$ regions. Thus, the β -hairpin structure is formed more at the interface.

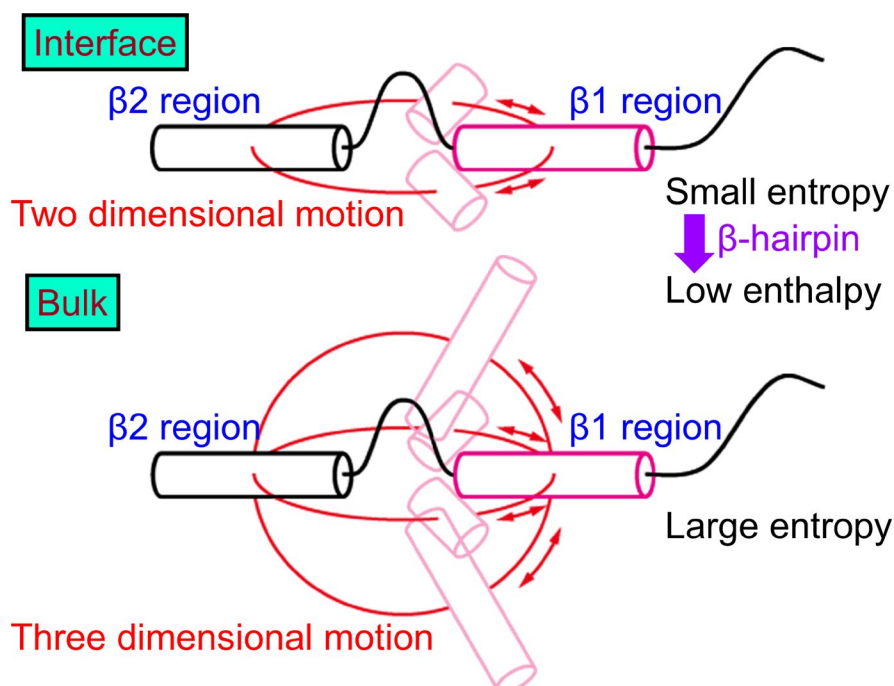


Figure 8 Schematic illustration of A β 40 at the air–water interface and in bulk water. Reproduced with permission from Ref. [27].

To illustrate the β -hairpin formation process in detail, the time series of snapshots are shown in Fig. 9. The initial conformation of A β 40 was fully extended (Fig. 9(a)). The β 1 and β 2 regions first formed helix structures, as shown in Fig. 9(b). These regions were stably bound to the interface and moved only at the interface. Then, the helix structure of the β 1 region was destroyed, as shown in Fig. 9(c), and the extended β 1 region approached the β 2 region, forming a β -bridge (Fig. 9(d)). The helix structure in the β 2 region was then destroyed, as shown in Fig. 9(e). The β -hairpin structure with more β -bridges was finally formed, as shown in Fig. 9(f). In this way, the hydrogen bonds between the β 1 and β 2 regions were formed step by step, and the structure changed from the helix structure to the extended structure.

In this simulation study, A β 40 took various conformations at the interface. To classify these conformations, principal component analysis (PCA) was performed. Figure 10(a) shows the free energy landscape for the first and second principal components of the system with the interface. Five local minimum states (States A–E) were observed. The typical structures of these states are shown in Fig. 11(a), where the N-terminal region D1–E11 was omitted for clarity because this region is flexible and has various conformations. The representative structure of each state is as follows. (State A) The β 1 and β 2 regions are close to each other. The β 1 region has an extended structure, and the β 2 region has a helix structure. A β -bridge is formed between these regions. (State B) The β 1 and β 2 regions are closer to each other than the structure at State A. Both regions have an extended structure, forming a stable β -hairpin structure. (State C) The β 1 region forms a helix structure while the β 2 region forms a β -bridge. Another β -bridge was formed near the linker region between the β 1 and β 2 regions. (State D) The β 1 region forms a β -hairpin structure, while the β 2 region forms a helix structure. No β -bridge is formed between the two regions. (State E) A β 40 takes a random coil structure and does not form a specific secondary structure.

Figure 10(b) shows the free energy landscapes for the first and second principal components obtained from the simulations in bulk water. Again, five local minimum states (States A'–E') are observed. Figure 11(b) shows a typical structure of A β peptide in bulk water. (State A') Both β 1 and β 2 regions do not form a secondary structure. (State B') Both the β 1 and β 2 regions have helix structures. (State C') A helix structure is formed in the β 2 region, while the β 1 region has a random coil structure. (State D') A β -bridge is formed in the β 2 region, while the β 1 region forms a helix structure. (State E') A β -sheet structure is formed between the β 1 and β 2 regions. A helix structure is formed in the linker region.

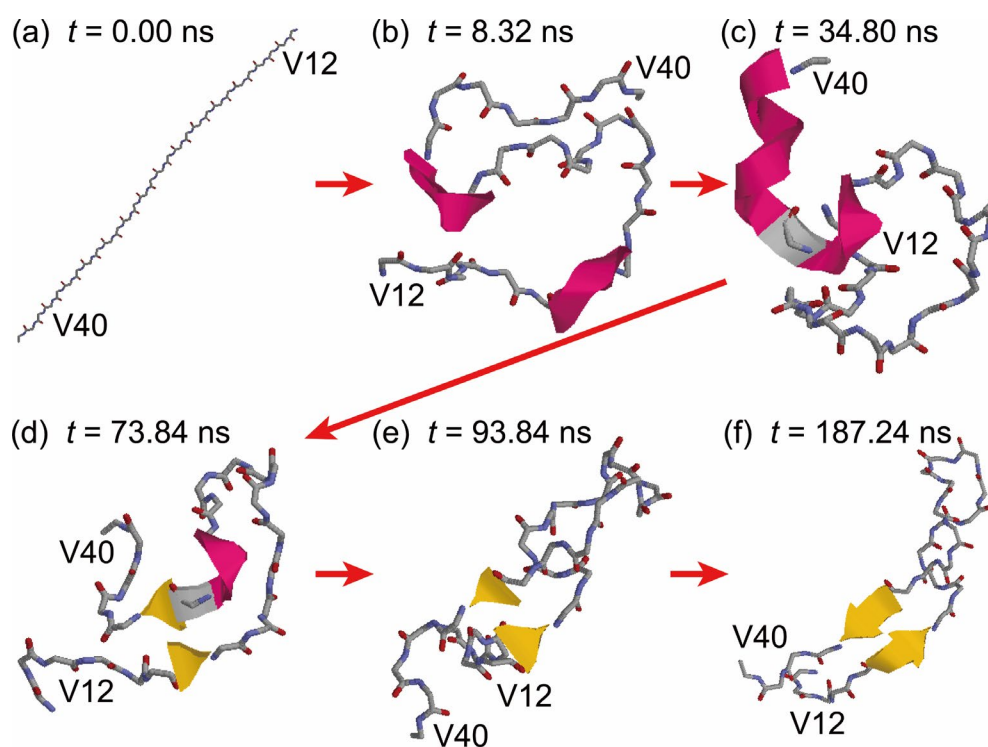


Figure 9 Time series of snapshots of A β 40 at the air–water interface. Residues D1–E11 are omitted for clarity. Reproduced with permission from Ref. [27].

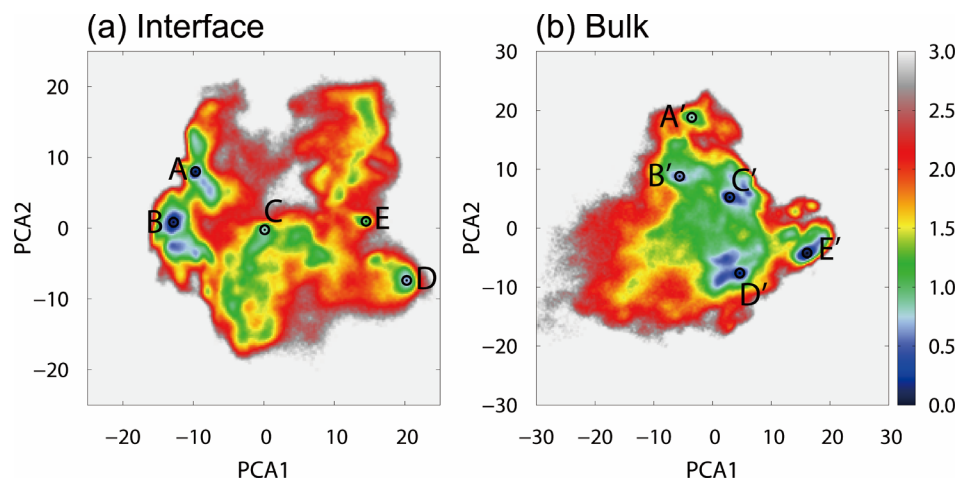


Figure 10 (a) The free energy landscape of A β 40 at the air–water interface. The local-minimum free-energy states are labeled as State A to State E. (b) The free energy landscape in bulk water. The local-minimum states are labeled as State A' to State E'. The horizontal and vertical axes are the first and second principal component axes, respectively. These axes were determined from (a) the MD simulations at the air–water interface and (b) those in bulk water. The unit of the free energy landscape is kcal/mol. Reproduced with permission from Ref. [27].

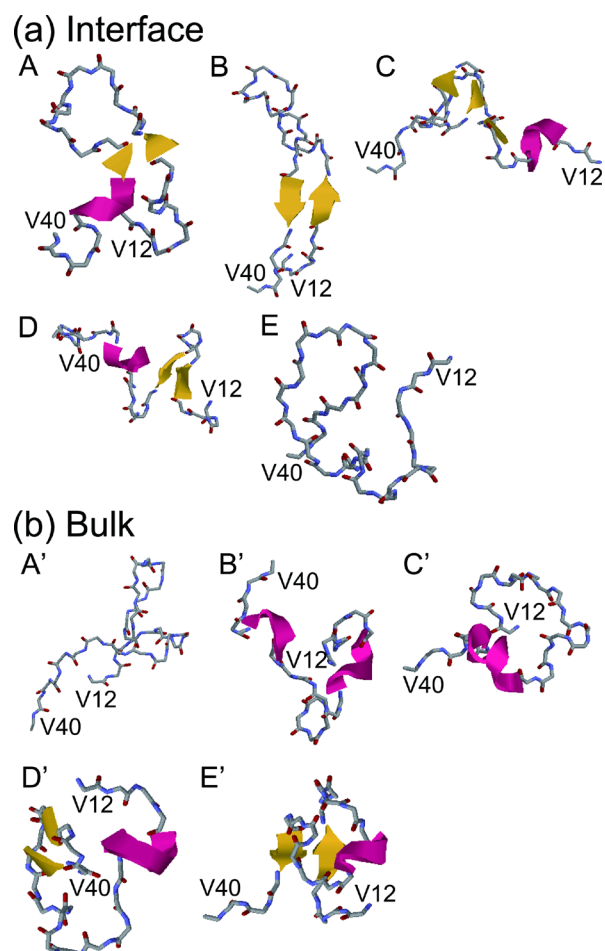


Table 1 Free energy and fractional population of States A–E at the interface and States A'–E' in bulk water [27].

| State | Free energy (kcal/mol) | Population (%) |
|-------|------------------------|----------------|
| A | 0.3 ± 0.4 | 10.3 ± 5.4 |
| B | 0.0 ± 0.3 | 17.5 ± 7.9 |
| C | 0.4 ± 0.3 | 8.3 ± 3.7 |
| D | 0.6 ± 0.8 | 6.4 ± 4.8 |
| E | 1.1 ± 0.3 | 2.7 ± 1.1 |
| A' | 1.0 ± 0.6 | 3.1 ± 2.2 |
| B' | 0.3 ± 0.4 | 9.8 ± 4.8 |
| C' | 0.1 ± 0.3 | 13.5 ± 5.3 |
| D' | 0.0 ± 0.2 | 16.8 ± 5.0 |
| E' | 0.4 ± 0.5 | 9.1 ± 5.6 |

Figure 11 Typical structures (a) at States A–E in Fig. 10(a) and (b) at States A'–E' in Fig. 10(b). Reproduced with permission from Ref. [27].

The free energy and fractional population of each state are listed in Table 1. The most stable state at the interface is State B, and the next stable state is State A. As shown in Fig. 11(a), both states form a β -hairpin structure between the β 1 and β 2 regions. On the other hand, the most stable state in bulk water is State D', in which a β -bridge is formed in the β 2 region, but no β -hairpin structure is formed between the β 1 and β 2 regions. The state E', in which the β -hairpin structure is formed between the β 1 and β 2 regions, is the fourth-lowest local-minimum free-energy state. These results indicate that A β 40 rarely forms the β -hairpin structure with the β 1 and β 2 regions in bulk water and that the probability of the β -hairpin structure at the interface is higher than in bulk water.

A β 40 Peptide on the GM1-Glycan Cluster

The last topic of this review is the conformational change of an A β peptide upon binding to a GM1-glycan cluster [34], which consists of a self-assembled supramolecule and GM1 glycans transplanted on it. The conformational change of A β upon interaction with the GM1 glycans is a subject of interest.

To prepare the initial conformations for the MD simulations, the GM1-glycan cluster and A β 40 were placed with a distance of 55 Å between their centers of mass in explicit water, as shown in Fig. 12. Nine different initial conditions were prepared like Fig. 12. After energy minimization, equilibration MD simulations were performed for 2 ns in the isothermal–isobaric ensemble at 300 K and 1 atm. Temperature and pressure were controlled by using the Langevin thermostat [143] and the Berendsen barostat [144], respectively. The production run was then performed for 1.5 μ s in the canonical ensemble from each initial condition. The temperature was set at 300 K so that it is the same as that in the experimental condition [97]. For comparison, MD simulations of an A β 40 monomer only were also performed in explicit water. Here, nine different initial conditions were prepared again. The canonical MD simulations were performed for 1.5 μ s from each initial condition. For more details of the simulations, please refer to Ref. [34].

As a result of the simulations, the spontaneous binding of A β to the GM1-glycan cluster was observed. It is also found that the HHQ region, which corresponds to residues 13–15, binds well to the GM1-glycan cluster. This fact is almost consistent with the results for the air–water interface, as we mentioned in the previous section that the β 1 region (residues 10–22) is present at the air–water interface. Furthermore, the HHQ region, unlike the other residues, was found to be attached to any of all sugar residues of the GM1-glycan cluster. Detailed structural analysis revealed that the five-membered rings of the histidine side chains in the HHQ region were stacked on the six-membered rings of the sugar residues, as shown in Fig. 13. These results suggest that the binding of A β to the GM1-glycan cluster is mainly stabilized by the stacking of the histidine side chains in the HHQ region with any sugar residues of the GM1-glycan moiety.

To clarify the structural characteristics of A β on the GM1-glycan cluster, the secondary structures of A β on the GM1-glycan cluster were compared with that of an A β monomer in bulk water with Define Secondary Structure of Proteins (DSSP) analysis. As shown in Fig. 14, an α -helix structure at residues 31–37 in the C-terminal region increases when A β is bound to the GM1-glycan cluster. This result is in good agreement with previous experimental studies, in which A β formed an α -helix structure at residues 31–36 on GM1 micelles [27].

It has been shown that on the GM1 clusters on the neuronal cell membranes, A β undergoes a conformational change to pathological aggregates after an increase in the α -helix structure [145]. Therefore, the α -helix formation can be considered as the first process of this structural change. Since the GM1-glycan moiety is the headgroup that exists above the lipid ceramide moiety (Fig. 2), this result suggests that the pathological conformational change of A β has already started in the GM1-glycan moiety and that A β then moves to the lipid interface. It was proposed that this α -helix formation of A β occurs in two steps as follows.

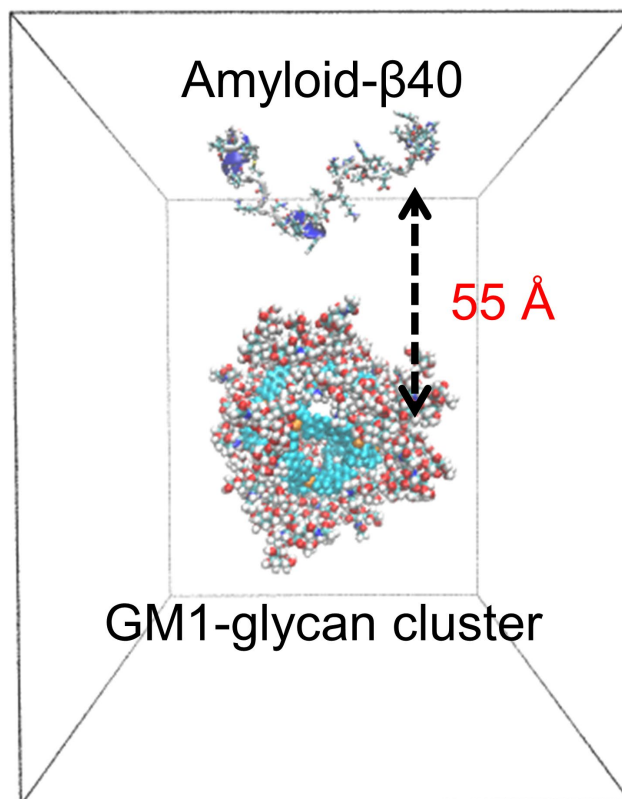


Figure 12 An initial structure used in the MD simulations of the A β 40 peptide and GM1-glycan cluster. Reproduced with permission from Ref. [34].

Step 1: In the monomeric state in water, the C-terminus of A β and Lys28 form a salt bridge. At this time, the C-terminal region forms a turn, bend, or β -sheet structure. Such conformations correspond to State D' in Fig. 11(b), which is the most stable state of A β in bulk water.

Step 2: When A β binds to the GM1-glycan cluster, Lys28 also forms a salt bridge with Neu in the GM1-glycan moiety, preventing the formation of a salt bridge with the C-terminus. Therefore, the C-terminal region is hydrated, and then the α -helix increases.

A schematic illustration of these two steps is shown in Fig. 15. The above results show that the α -helix formation is the first step in the structural change that leads to the pathological aggregation. Preventing this structural change may be a strategy for developing a preventive drug for Alzheimer's disease.

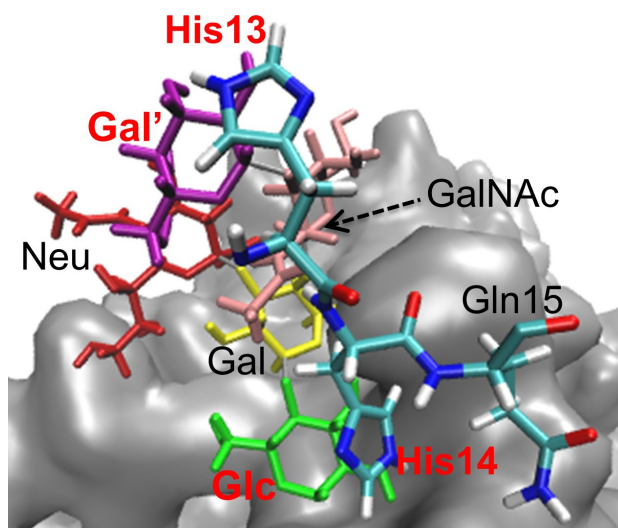


Figure 13 Stacking of the HHQ (13-15) region to the GM1-glycan moiety. The sugar and amino-acid residues that are stacked are shown in red. Reproduced with permission from Ref. [34].

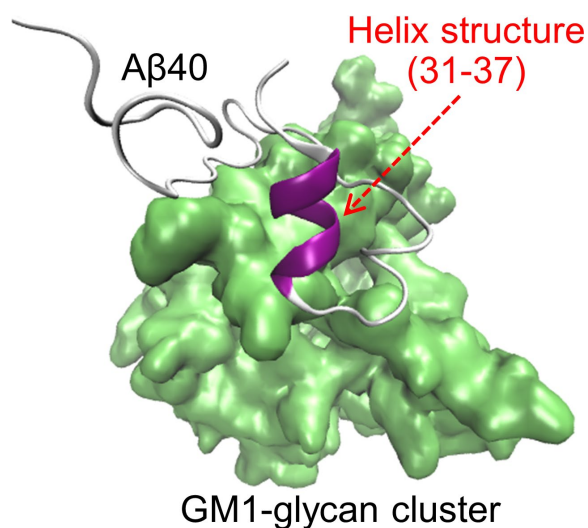


Figure 14 A typical snapshot of A β 40 with the α -helix structure formed in residues 31–37. Reproduced with permission from Ref. [34].

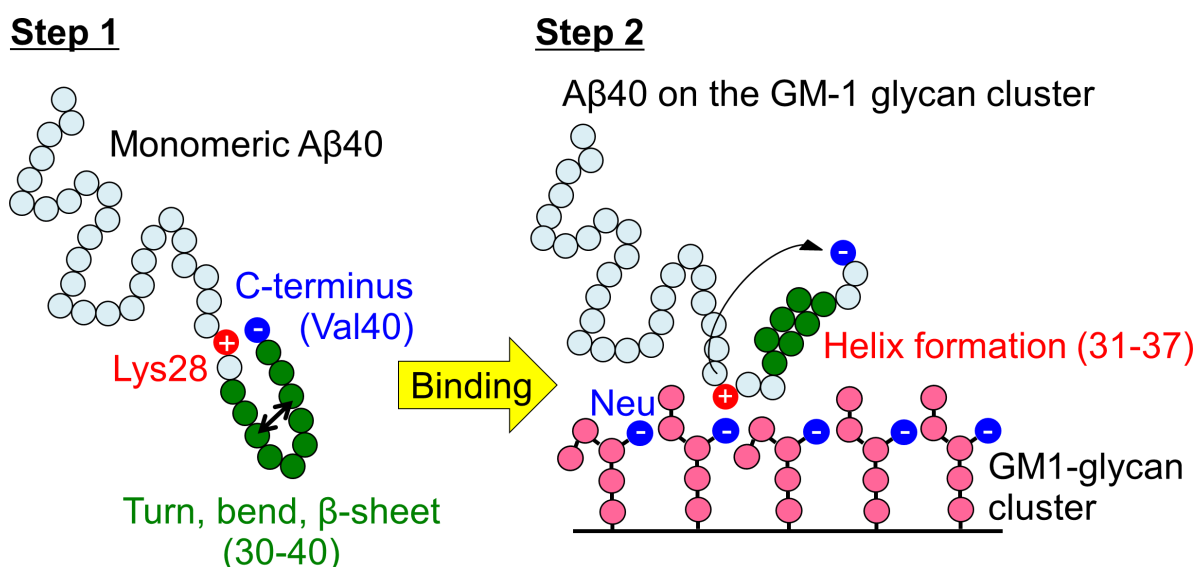


Figure 15 Schematic illustration of the mechanism of conformational change of A β 40 upon binding to the GM1-glycan cluster. Step 1 and Step 2 represent before and after binding, respectively. Reproduced with permission from Ref. [34].

As described in the previous section, at the air–water interface, A β first formed the α -helix structure in the C-terminal region and then formed the β -hairpin structure between the β 1 and β 2 regions (Fig. 9). However, on the GM1-glycan cluster, A β formed the α -helix structure in the C-terminal region, but did not form the β -hairpin structure between the β 1 and β 2 regions. In other words, we can regard that A β on the GM1-glycan cluster reached only a conformation that corresponds to Fig. 9(c) at the air–water interface. The reason for this difference can be considered as follows. Unlike the GM1 clusters on the neuronal cell membrane, the GM1-glycan moiety on the self-assembled supramolecule has low fluidity. A β can reach only the GM1-glycan moiety that corresponds to the headgroup of the GM1 cluster on the membrane because the low fluidity makes A β trapped at the GM1-glycan moiety. The GM1-glycan moiety is relatively hydrophilic, and the difference between hydrophobicity and hydrophilicity at the interface between the GM1-glycan region and the aqueous solution is smaller than that at the air–water interface. The reason for the formation of the β -hairpin structure is that the β 1 and β 2 regions are constrained at the interface, as shown in Fig. 8. However, the GM1-glycan moieties of the GM1-glycan cluster do not constrain the β 1 and β 2 regions as much as the air–water interface. Therefore, it is considered that the β -hairpin structure was not formed on the GM1-glycan cluster. By performing MD simulations for A β with the GM1 clusters on the neuronal cell membrane in the future, it is expected that A β peptides can reach the interface between the GM1-glycan moiety and the lipid-ceramide moiety and form the β -hairpin structure. Further research progress is awaited.

Conclusions

In this review, we described the recent MD simulations of the A β peptides in the heterogeneous environments. The A β (16–22) fragments and A β 40 peptides tend to exist at hydrophilic/hydrophobic interfaces, such as the neuronal cell membrane surface and air–water interface because these peptides have both hydrophilic and hydrophobic residues. Therefore, the concentration of the A β peptides is high at the interface. This is one of the factors that promote the aggregation at the interface. In addition, after A β 40 forms the α -helix structure, the β 1 and β 2 regions approach each other to form the β -hairpin structure. This β -hairpin structure is rarely formed in bulk water. It is known in previous studies that the β -hairpin structure plays an important role in oligomer formation because the β -hairpin structure enhances the oligomer formation with intermolecular β -sheet structures. Thus, not only because the concentration of the A β peptides is higher at the interface, but also because the β -hairpin structure is formed more, A β oligomers are formed more at the interface than in bulk water. The reason of the β -hairpin formation is as follows. The β 1 and β 2 regions can only move in two dimensions, and the entropy of A β at the interface is smaller than in bulk water. To reduce the free energy, the enthalpy must be reduced. The enthalpy is reduced by the formation of hydrogen bonds between the β 1 and β 2 regions. The β -hairpin structure is thus formed.

In addition to the air–water interface, we reviewed the conformational changes of the A β 40 peptide on the GM1-glycan cluster, which is composed of a self-assembled supramolecule and GM1-glycan moieties transplanted on it. When A β 40 binds to the GM1-glycan cluster, the 13th–15th residues (HHQ region) stack against any glycan residue. This interaction contributes to the stabilization of A β 40 on the GM1-glycan cluster. The binding to the GM1-glycan cluster stabilizes the α -helix structure in the C-terminal region of A β . The helix structure is formed in the following two steps. (1) In the monomeric state in water, the C-terminus of A β and Lys28 form a salt bridge while the C-terminal region forms a turn, bend, or β -sheet structure. (2) When A β binds to the GM1-glycan cluster, Lys28 forms a salt bridge with Neu in the GM1-glycan moiety, preventing the formation of a salt bridge with the C-terminus. Therefore, the C-terminal region is hydrated, and then the α -helix structure increases. These results suggest that the α -helix formation, the first pathological structural change of A β , has already started when A β binds to the GM1-glycan moiety.

In this way, the MD simulations have revealed the conformational change process of the A β peptides in the heterogeneous environments. Furthermore, it has been elucidated which atom or amino-acid residue plays an important role. These studies will enhance our physicochemical understanding of the structural changes of A β at the interface and the mechanism of Alzheimer's disease pathogenesis. We hope that MD simulation will be a tool for developing treatments for neurodegenerative diseases such as Alzheimer's disease in the future.

Conflict of Interest

The authors declare no conflict of interests.

Author Contributions

Y. T., S. G. I., and H. O. wrote the manuscript.

Acknowledgements

We gratefully thank all collaborators of the works described in this review. These works were supported by JSPS KAKENHI (Grant No. JP16H00790, JP24740296, and JP26102550). Computations in this review were performed using supercomputers at the Research Center for Computational Science, Okazaki Research Facilities, National Institutes of Natural Sciences, Japan.

References

- [1] Sipe, J. D., Cohen, A. S., Review: History of the amyloid fibril. *J. Struct. Biol.* 130, 88-98 (2000). <https://doi.org/10.1006/jsbi.2000.4221>
- [2] Chiti, F., Dobson, C. M., Protein misfolding, functional amyloid, and human disease. *Annu. Rev. Biochem.* 75, 333-366 (2006). <https://doi.org/10.1146/annurev.biochem.75.101304.123901>
- [3] Chiti, F., Dobson, C. M., Amyloid formation by globular proteins under native conditions. *Nat. Chem. Biol.* 5, 15-22 (2009). <https://doi.org/10.1038/nchembio.131>
- [4] Knowles, T. P., Vendruscolo, M., Dobson, C. M. The amyloid state and its association with protein misfolding diseases. *Nat. Rev. Mol. Cell Biol.* 15, 384-396 (2014). <https://doi.org/10.1038/nrm3810>
- [5] Tycko, R. Amyloid polymorphism: structural basis and neurobiological relevance. *Neuron* 86, 632-645 (2015). <https://doi.org/10.1016/j.neuron.2015.03.017>
- [6] Petkova, A. T., Ishii, Y., Balbach, J. J., Antzutkin, O. N., Leapman, R. D., Delaglio, F., et al. A structural model for Alzheimer's β -amyloid fibrils based on experimental constraints from solid state NMR. *Proc. Natl. Acad. Sci. U.S.A.* 99, 16742-16747 (2002). <https://doi.org/10.1073/pnas.262663499>
- [7] Lührs, T., Ritter, C., Adrian, M., Riek-Loher, D., Bohrmann, B., Dobeli, H., et al. 3D structure of Alzheimer's amyloid- β (1-42) fibrils. *Proc. Natl. Acad. Sci. U.S.A.* 102, 17342-17347 (2005). <https://doi.org/10.1073/pnas.0506723102>
- [8] Petkova, A. T., Yau, W. M., Tycko, R. Experimental constraints on quaternary structure in Alzheimer's β -amyloid fibrils. *Biochemistry* 45, 498-512 (2006). <https://doi.org/10.1021/bi051952q>
- [9] Bernstein, S. L., Dupuis, N. F., Lazo, N. D., Wytenbach, T., Condron, M. M., Bitan, G., et al. Amyloid- β protein oligomerization and the importance of tetramers and dodecamers in the aetiology of Alzheimer's disease. *Nat. Chem.* 1, 326-331 (2009). <https://doi.org/10.1038/nchem.247>
- [10] Baftizadeh, F., Pietrucci, F., Biarnes, X., Laio, A. Nucleation process of a fibril precursor in the C-terminal segment of amyloid- β . *Phys. Rev. Lett.* 110, 168103 (2013). <https://doi.org/10.1103/PhysRevLett.110.168103>
- [11] Lu, J. X., Qiang, W., Yau, W. M., Schwieters, C. D., Meredith, S. C., Tycko, R. Molecular Structure of β -Amyloid Fibrils in Alzheimer's Disease Brain Tissue. *Cell* 154, 1257-1268 (2013). <https://doi.org/10.1016/j.cell.2013.08.035>
- [12] Sarkar, B., Mithu, V. S., Chandra, B., Mandal, A., Chandrakesan, M., Bhowmik, D., et al. Significant structural differences between transient amyloid- β oligomers and less-toxic fibrils in regions known to harbor familial Alzheimer's mutations. *Angew. Chem. Int. Ed.* 53, 6888-6892 (2014). <https://doi.org/10.1002/anie.201402636>
- [13] Xiao, Y., Ma, B., McElheny, D., Parthasarathy, S., Long, F., Hoshi, M., et al. $A\beta$ (1-42) fibril structure illuminates self-recognition and replication of amyloid in Alzheimer's disease. *Nat. Struct. Mol. Biol.* 22, 499-505 (2015). <https://doi.org/10.1038/nsmb.2991>
- [14] Gremer, L., Schölzel, D., Schenk, C., Reinartz, E., Labahn, J., Ravelli, R. B. G., et al. Fibril structure of amyloid- β (1-42) by cryoelectron microscopy. *Science* 358, 116 (2017). <https://doi.org/10.1126/science.aao2825>
- [15] Ilie, I. M., Caffisch, A., Simulation studies of amyloidogenic polypeptides and their aggregates. *Chem. Rev.* 119, 6956-6993 (2019). <https://doi.org/10.1021/acs.chemrev.8b00731>
- [16] Nguyen, P. H., Derreumaux, P. Structures of the intrinsically disordered $A\beta$, tau and α -synuclein proteins in aqueous solution from computer simulations. *Biophys. Chem.* 264, 106421 (2020). <https://doi.org/10.1016/j.bpc.2020.106421>
- [17] Itoh, S. G., Okumura, H., Promotion and inhibition of amyloid- β peptide aggregation: Molecular dynamics studies. *Int. J. Mol. Sci.* 22, 1859 (2021). <https://doi.org/10.3390/ijms22041859>
- [18] Strodel, B. Amyloid aggregation simulations: Challenges, advances and perspectives. *Curr. Opin. Struct. Biol.* 67, 145-152 (2021). <https://doi.org/10.1016/j.sbi.2020.10.019>
- [19] Glenner, G. G., Wong, C. W. Alzheimer's disease: Initial report of the purification and characterization of a novel cerebrovascular amyloid protein. *Biochem. Biophys. Res. Commun.* 120, 885-890 (1984). [https://doi.org/10.1016/s0006-291x\(84\)80190-4](https://doi.org/10.1016/s0006-291x(84)80190-4)
- [20] Masters, C. L., Simms, G., Weinman, N. A., Multhaup, G., McDonald, B. L., Beyreuther, K. Amyloid plaque core protein in Alzheimer disease and Down syndrome. *Proc. Natl. Acad. Sci. U.S.A.* 82, 4245-4249 (1985).

- <https://doi.org/10.1073/pnas.82.12.4245>
- [21] Hardy, J., Selkoe, D. J. The amyloid hypothesis of Alzheimer's disease: progress and problems on the road to therapeutics. *Science* 297, 353-356 (2002). <https://doi.org/10.1126/science.1072994>
- [22] Kaye, R., Head, E., Thompson, J. L., McIntire, T. M., Milton, S. C., Cotman, C. W., et al. Common structure of soluble amyloid oligomers implies common mechanism of pathogenesis. *Science* 300, 486-489 (2003). <https://doi.org/10.1126/science.1079469>
- [23] Haass, C., Selkoe, D. J. Soluble protein oligomers in neurodegeneration: Lessons from the Alzheimer's amyloid β -peptide. *Nat. Rev. Mol. Cell Biol.* 8, 101-112 (2007). <https://doi.org/10.1038/nrm2101>
- [24] Shankar, G. M., Li, S. M., Mehta, T. H., Garcia-Munoz, A., Shepardson, N. E., Smith, I., et al. Amyloid- β protein dimers isolated directly from Alzheimer's brains impair synaptic plasticity and memory. *Nat. Med.* 14, 837-842 (2008). <https://doi.org/10.1038/nm1782>
- [25] Morinaga, A., Hasegawa, K., Nomura, R., Ookoshi, T., Ozawa, D., Goto, Y., et al. Critical role of interfaces and agitation on the nucleation of A β amyloid fibrils at low concentrations of A β monomers. *Biochim. Biophys. Acta* 1804, 986-995 (2010). <https://doi.org/10.1016/j.bbapap.2010.01.012>
- [26] Jean, L., Lee, C. F., Vaux, D. J., Enrichment of Amyloidogenesis at an Air-Water Interface. *Biophys. J.* 102, 1154-1162 (2012). <https://doi.org/10.1016/j.bpj.2012.01.041>
- [27] Itoh, S. G., Yagi-Utsumi, M., Kato, K., Okumura, H. Effects of a hydrophilic/hydrophobic interface on amyloid- β peptides studied by molecular dynamics simulations and NMR experiments. *J. Phys. Chem. B* 123, 160-169 (2019). <https://doi.org/10.1021/acs.jpcc.8b11609>
- [28] Yagi-Utsumi, M., Kato, K., Nishimura, K. Membrane-induced dichotomous conformation of amyloid β with the disordered N-terminal segment followed by the stable C-terminal β structure. *PLoS One* 11, e0146405 (2016). <https://doi.org/10.1371/journal.pone.0146405>
- [29] Fantini, J., Yahi, N., Molecular insights into amyloid regulation by membrane cholesterol and sphingolipids: common mechanisms in neurodegenerative diseases. *Expert Rev. Mol. Med.* 12, e27 (2010). <https://doi.org/10.1017/S1462399410001602>
- [30] Kakio, A., Nishimoto, S., Yanagisawa, K., Kozutsumi, Y. Interactions of amyloid β -protein with various gangliosides in raft-like membranes: importance of GM1 ganglioside-bound form as an endogenous seed for Alzheimer amyloid. *Biochemistry* 41, 7385-7390 (2002). <https://doi.org/10.1021/bi0255874>
- [31] Hayashi, H., Kimura, N., Yamaguchi, H., Hasegawa, K., Yokoseki, T., Shibata, M., et al. A seed for Alzheimer amyloid in the brain. *J. Neurosci.* 24, 4894-4902 (2004). <https://doi.org/10.1523/JNEUROSCI.0861-04.2004>
- [32] Tachi, Y., Okumura, H. Structural changes in amyloid- β by binding to glycan clusters. *SEIBUTSU BUTSURI* 61, 186-188 (2021). <https://doi.org/10.2142/biophys.61.186>
- [33] Okumura, H., Itoh, S. G. Molecular dynamics simulations of amyloid- β (16-22) peptide aggregation at air-water interfaces. *J. Chem. Phys.* 152, 095101 (2020). <https://doi.org/10.1063/1.5131848>
- [34] Tachi, Y., Okamoto, Y., Okumura, H. Conformational change of amyloid- β 40 in association with binding to GM1-glycan cluster. *Sci. Rep.* 9, 6853 (2019). <https://doi.org/10.1038/s41598-019-43117-6>
- [35] Allison, J. R., Varnai, P., Dobson, C. M., Vendruscolo, M. Determination of the free energy landscape of α -synuclein using spin label nuclear magnetic resonance measurements. *J. Am. Chem. Soc.* 131, 18314 (2009). <https://doi.org/10.1021/ja904716h>
- [36] Sgourakis, N. G., Merced-Serrano, M., Boutsidis, C., Drineas, P., Du, Z., Wang, C., et al. Atomic-Level characterization of the ensemble of the A β (1-42) monomer in water using unbiased molecular dynamics simulations and spectral algorithms. *J. Mol. Biol.* 405, 570 (2011). <https://doi.org/10.1016/j.jmb.2010.10.015>
- [37] Velez-Vega, C., Escobedo, F. A. Characterizing the structural behavior of selected A β -42 monomers with different solubilities. *J. Phys. Chem. B* 115, 4900-4910 (2011). <https://doi.org/10.1021/jp1086575>
- [38] Olubiyi, O. O., Strodel, B. Structures of the amyloid β -peptides. A β 1-40 and A β 1-42 as influenced by pH and a d-peptide. *J. Phys. Chem. B* 116, 3280 (2012). <https://doi.org/10.1021/jp2076337>
- [39] Itoh, S. G., Okumura, H. Hamiltonian replica-permutation method and its applications to an alanine dipeptide and amyloid- β (29-42) peptides. *J. Comput. Chem.* 34, 2493-2497 (2013). <https://doi.org/10.1002/jcc.23402>
- [40] Itoh, S. G., Okumura, H. Coulomb replica-exchange method: Handling electrostatic attractive and repulsive forces for biomolecules. *J. Comput. Chem.* 34, 622-639 (2013). <https://doi.org/10.1002/jcc.23167>
- [41] Rosenman, D. J., Connors, C. R., Chen, W., Wang, C., Garcia, A. E. A β monomers transiently sample oligomer and fibril-like configurations: Ensemble characterization using a combined MD/NMR approach. *J. Mol. Biol.* 425, 3338 (2013). <https://doi.org/10.1016/j.jmb.2013.06.021>
- [42] Rosenman, D. J., Wang, C., Garcia, A. E. Characterization of A β monomers through the convergence of ensemble properties among simulations with multiple force fields. *J. Phys. Chem. B* 120, 259 (2016). <https://doi.org/10.1021/acs.jpcc.5b09379>
- [43] Ilie, I. M., Nayar, D., den Otter, W. K., van der Vegt, N. F. A., Briels, W. J. Intrinsic conformational preferences

- and interactions in α -synuclein fibrils: Insights from molecular dynamics simulations. *J. Chem. Theory Comput.* 14, 3298-3310 (2018). <https://doi.org/10.1021/acs.jctc.8b00183>
- [44] Itoh, S. G., Okamoto, Y. Amyloid- β (29-42) dimer formations studied by a multicanonical-multioverlap molecular dynamics simulation. *J. Phys. Chem. B* 112, 2767-2770 (2008). <https://doi.org/10.1021/jp712170h>
- [45] Chebaro, Y., Mousseau, N., Derreumaux, P. Structures and thermodynamics of Alzheimer's amyloid- β A β (16-35) monomer and dimer by replica exchange molecular dynamics simulations: Implication for full-length A β fibrillation. *J. Phys. Chem. B* 113, 7668-7675 (2009). <https://doi.org/10.1021/jp900425e>
- [46] Cote, S., Laghaei, R., Derreumaux, P., Mousseau, N. Distinct dimerization for various alloforms of the amyloid- β protein: A β (1-40), A β (1-42), and A β (1-40)(D23N). *J. Phys. Chem. B* 116, 4043-4055 (2012). <https://doi.org/10.1021/jp2126366>
- [47] Chiang, H. L., Chen, C. J., Okumura, H., Hu, C. K. Transformation between α -helix and β -sheet structures of one and two polyglutamine peptides in explicit water molecules by replica-exchange molecular dynamics simulations. *J. Comput. Chem.* 35, 1430-1437 (2014). <https://doi.org/10.1002/jcc.23633>
- [48] Itoh, S. G., Okumura, H. Dimerization process of amyloid- β (29-42) studied by the Hamiltonian replica-permutation molecular dynamics simulations. *J. Phys. Chem. B* 118, 11428-11436 (2014). <https://doi.org/10.1021/jp505984e>
- [49] Nguyen, P. H., Sterpone, F., Campanera, J. M., Nasica-Labouze, J., Derreumaux, P. Impact of the A2V mutation on the heterozygous and homozygous A β 1-40 dimer structures from atomistic simulations. *ACS Chem. Neurosci.* 7, 823-832 (2016). <https://doi.org/10.1021/acschemneuro.6b00053>
- [50] Tarus, B., Tran, T. T., Nasica-Labouze, J., Sterpone, F., Nguyen, P. H., Derreumaux, P. Structures of the Alzheimer's wild-type A β 1-40 dimer from atomistic simulations. *J. Phys. Chem. B* 119, 10478-10487 (2015). <https://doi.org/10.1021/acs.jpcc.5b05593>
- [51] Nguyen, P. H., Sterpone, F., Pouplana, R., Derreumaux, P., Campanera, J. M. Dimerization mechanism of Alzheimer A β 40 peptides: The high content of intrapeptide-stabilized conformations in A2V and A2T heterozygous dimers retards amyloid fibril formation. *J. Phys. Chem. B* 120, 12111-12126 (2016). <https://doi.org/10.1021/acs.jpcc.6b10722>
- [52] Das, P., Chacko, A. R., Belfort, G., Alzheimer's protective cross-interaction between wild-type and A2T variants alters A β 42 dimer structure. *ACS Chem. Neurosci.* 8, 606 (2017). <https://doi.org/10.1021/acschemneuro.6b00357>
- [53] Man, V. H., Nguyen, P. H., Derreumaux, P. Conformational ensembles of the wild-type and S8C A β 1-42 dimers. *J. Phys. Chem. B* 121, 2434-2442 (2017). <https://doi.org/10.1021/acs.jpcc.7b00267>
- [54] Man, V. H., Nguyen, P. H., Derreumaux, P. High-resolution structures of the amyloid- β 1-42 dimers from the comparison of four atomistic force fields. *J. Phys. Chem. B* 121, 5977-5987 (2017). <https://doi.org/10.1021/acs.jpcc.7b04689>
- [55] Sharma, B., Ranganathan, S. V., Belfort, G. Weaker N-terminal interactions for the protective over the causative A β peptide dimer mutants. *ACS Chem. Neurosci.* 9, 1247-1253 (2018). <https://doi.org/10.1021/acschemneuro.7b00412>
- [56] Nishizawa, H., Okumura, H. Classical molecular dynamics simulation to understand role of a zinc ion for aggregation of amyloid- β peptides. *J. Comput. Chem., Jpn.* 17, 76-79 (2018). <https://doi.org/10.2477/jccj.2018-0005>
- [57] Yamauchi, M., Okumura, H. Dimerization of α -synuclein fragments studied by isothermal-isobaric replica-permutation molecular dynamics simulation. *J. Chem. Inf. Model.* 61, 1307-1321 (2021). <https://doi.org/10.1021/acs.jcim.0c01056>
- [58] Gsponer, J., Haberthur, U., Caflisch, A. The role of side-chain interactions in the early steps of aggregation: Molecular dynamics simulations of an amyloid-forming peptide from the yeast prion Sup35. *Proc. Natl. Acad. Sci. U.S.A.* 100, 5154-5159 (2003). <https://doi.org/10.1073/pnas.0835307100>
- [59] Urbanc, B., Betnel, M., Cruz, L., Bitan, G., Teplow, D. B. Elucidation of amyloid β -protein oligomerization mechanisms: Discrete molecular dynamics study. *J. Am. Chem. Soc.* 132, 4266-4280 (2010). <https://doi.org/10.1021/ja9096303>
- [60] Riccardi, L., Nguyen, P. H., Stock, G. Construction of the free energy landscape of peptide aggregation from molecular dynamics simulations. *J. Chem. Theory Comput.* 8, 1471-1479 (2012). <https://doi.org/10.1021/ct200911w>
- [61] Carballo-Pacheco, M., Ismail, A. E., Strodel, B. Oligomer formation of toxic and functional amyloid peptides studied with atomistic simulations. *J. Phys. Chem. B* 119, 9696-9705 (2015). <https://doi.org/10.1021/acs.jpcc.5b04822>
- [62] Itoh, S. G., Okumura, H. Oligomer formation of amyloid- β (29-42) from its monomers using the Hamiltonian replica-permutation molecular dynamics simulation. *J. Phys. Chem. B* 120, 6555-6561 (2016).

- <https://doi.org/10.1021/acs.jpcb.6b03828>
- [63] Sun, Y., Wang, B., Ge, X., Ding, F. Distinct oligomerization and fibrillization dynamics of amyloid core sequences of amyloid- β and islet amyloid polypeptide. *Phys. Chem. Chem. Phys.* 19, 28414-28423 (2017). <https://doi.org/10.1039/c7cp05695h>
- [64] Barz, B., Liao, Q., Strodel, B. Pathways of amyloid- β aggregation depend on oligomer shape. *J. Am. Chem. Soc.* 140, 319 (2018). <https://doi.org/10.1021/jacs.7b10343>
- [65] Ge, X., Sun, Y., Ding, F. Structures and dynamics of β -barrel oligomer intermediates of amyloid- β 16-22 aggregation. *Biochim. Biophys. Acta* 1860, 1687-1697 (2018). <https://doi.org/10.1016/j.bbamem.2018.03.011>
- [66] Sun, Y., Ge, X., Xing, Y., Wang, B., Ding, F. β -barrel oligomers as common intermediates of peptides self-assembling into cross- β aggregates. *Sci. Rep.* 8, 10353 (2018). <https://doi.org/10.1038/s41598-018-28649-7>
- [67] Nguyen, P. H., Li, M. S., Stock, G., Straub, J. E., Thirumalai, D. Monomer adds to preformed structured oligomers of A β -peptides by a two-stage dock-lock mechanism. *Proc. Natl. Acad. Sci. U.S.A.* 104, 111-116 (2007). <https://doi.org/10.1073/pnas.0607440104>
- [68] O'Brien, E. P., Okamoto, Y., Straub, J. E., Brooks, B. R., Thirumalai, D. Thermodynamic perspective on the dock-lock growth mechanism of amyloid fibrils. *J. Phys. Chem. B* 113, 14421-14430 (2009). <https://doi.org/10.1021/jp9050098>
- [69] Takeda, T., Klimov, D. K. Probing energetics of A β fibril elongation by molecular dynamics simulations. *Biophys. J.* 96, 4428-4437 (2009). <https://doi.org/10.1016/j.bpj.2009.03.015>
- [70] Takeda, T., Klimov, D. K. Replica exchange simulations of the thermodynamics of A β fibril growth. *Biophys. J.* 96, 442-452 (2009). <https://doi.org/10.1016/j.bpj.2008.10.008>
- [71] Reddy, A. S., Wang, L., Singh, S., Ling, Y. L., Buchanan, L., Zanni, M. T., et al. Stable and metastable states of human amylin in solution. *Biophys. J.* 99, 2208-2216 (2010). <https://doi.org/10.1016/j.bpj.2010.07.014>
- [72] Han, M., Hansmann, U. H. Replica exchange molecular dynamics of the thermodynamics of fibril growth of Alzheimer's A β 42 peptide. *J. Chem. Phys.* 135, 065101 (2011). <https://doi.org/10.1063/1.3617250>
- [73] Straub, J. E., Thirumalai, D. Toward a molecular theory of early and late events in monomer to amyloid fibril formation. *Annu. Rev. Phys. Chem.* 62, 437-463 (2011). <https://doi.org/10.1146/annurev-physchem-032210-103526>
- [74] Gurry, T., Stultz, C. M. Mechanism of amyloid- β fibril elongation. *Biochemistry* 53, 6981-6991 (2014). <https://doi.org/10.1021/bi500695g>
- [75] Han, W., Schulten, K. Fibril elongation by A β 17-42: Kinetic network analysis of hybrid-resolution molecular dynamics simulations. *J. Am. Chem. Soc.* 136, 12450 (2014). <https://doi.org/10.1021/ja507002p>
- [76] Schwierz, N., Frost, C. V., Geissler, P. L., Zacharias, M. Dynamics of seeded A β 40-fibril growth from atomistic molecular dynamics simulations: Kinetic trapping and reduced water mobility in the locking step. *J. Am. Chem. Soc.* 138, 527-539 (2016). <https://doi.org/10.1021/jacs.5b08717>
- [77] Sasmal, S., Schwierz, N., Head-Gordon, T. Mechanism of nucleation and growth of A β 40 fibrils from all-atom and coarse-grained simulations. *J. Phys. Chem. B* 120, 12088-12097 (2016). <https://doi.org/10.1021/acs.jpcb.6b09655>
- [78] Bacci, M., Vymetal, J., Mihajlovic, M., Caflisch, A., Vitalis, A. Amyloid β fibril elongation by monomers involves disorder at the tip. *J. Chem. Theory Comput.* 13, 5117 (2017). <https://doi.org/10.1021/acs.jctc.7b00662>
- [79] Ilie, I. M., den Otter, W. K., Briels, W. J. The attachment of α -synuclein to a fiber: A coarse-grain approach. *J. Chem. Phys.* 146, 115102 (2017). <https://doi.org/10.1063/1.4978297>
- [80] Buchete, N. V., Tycko, R., Hummer, G. Molecular dynamics simulations of Alzheimer's β -amyloid protofilaments. *J. Mol. Biol.* 353, 804-821 (2005). <https://doi.org/10.1016/j.jmb.2005.08.066>
- [81] Baumketner, A., Krone, M. G., Shea, J. E. Role of the familial Dutch mutation E22Q in the folding and aggregation of the 15-28 fragment of the Alzheimer amyloid- β protein. *Proc. Natl. Acad. Sci. U.S.A.* 105, 6027-6032 (2008). <https://doi.org/10.1073/pnas.0708193105>
- [82] Lemkul, J. A., Bevan, D. R. Assessing the stability of Alzheimer's amyloid protofibrils using molecular dynamics. *J. Phys. Chem. B* 114, 1652 (2010). <https://doi.org/10.1021/jp9110794>
- [83] Okumura, H., Itoh, S. G. Structural and fluctuational difference between two ends of A β amyloid fibril: MD simulations predict only one end has open conformations. *Sci. Rep.* 6, 38422 (2016). <https://doi.org/10.1038/srep38422>
- [84] Rodriguez, R. A., Chen, L. Y., Plascencia-Villa, G., Perry, G. Thermodynamics of amyloid- β fibril elongation: Atomistic details of the transition state. *ACS Chem. Neurosci.* 9, 783-789 (2018). <https://doi.org/10.1021/acscchemneuro.7b00409>
- [85] Davidson, D. S., Brown, A. M., Lemkul, J. A. Insights into stabilizing forces in amyloid fibrils of differing sizes from polarizable molecular dynamics simulations. *J. Mol. Biol.* 430, 3819 (2018). <https://doi.org/10.1016/j.jmb.2018.05.020>

- [86] Ilie, I. M., Caflisch, A. Disorder at the tips of a disease-relevant A β 42 amyloid fibril: A molecular dynamics study. *J. Phys. Chem. B* 122, 11072 (2018). <https://doi.org/10.1021/acs.jpcc.8b05236>
- [87] Sun, Y., Qian, Z., Wei, G. The inhibitory mechanism of a fullerene derivative against amyloid- β peptide aggregation: An atomistic simulation study. *Phys. Chem. Chem. Phys.* 18, 12582-12591 (2016). <https://doi.org/10.1039/c6cp01014h>
- [88] Ngoc, L. L. N., Itoh, S. G., Sompornpisut, P., Okumura, H. Replica-permutation molecular dynamics simulations of an amyloid- β (16–22) peptide and polyphenols. *Chem. Phys. Lett.* 758, 137913 (2020). <https://doi.org/10.1016/j.cplett.2020.137913>
- [89] Okumura, H., Itoh, S. G. Amyloid fibril disruption by ultrasonic cavitation: Nonequilibrium molecular dynamics simulations. *J. Am. Chem. Soc.* 136, 10549-10552 (2014). <https://doi.org/10.1021/ja502749f>
- [90] Hoang Viet, M., Derreumaux, P., Li, M. S., Roland, C., Sagui, C., Nguyen, P. H. Picosecond dissociation of amyloid fibrils with infrared laser: A nonequilibrium simulation study. *J. Chem. Phys.* 143, 155101 (2015). <https://doi.org/10.1063/1.4933207>
- [91] Hoang Viet, M., Derreumaux, P., Nguyen, P. H. Nonequilibrium all-atom molecular dynamics simulation of the bubble cavitation and application to dissociate amyloid fibrils. *J. Chem. Phys.* 145, 174113 (2016). <https://doi.org/10.1063/1.4966263>
- [92] Okumura, H., Itoh, S. G., Nakamura, K., Kawasaki, T. Role of water molecules and helix structure stabilization in the laser-induced disruption of amyloid fibrils observed by nonequilibrium molecular dynamics simulations. *J. Phys. Chem. B* 125, 4964-4976 (2021). <https://doi.org/10.1021/acs.jpcc.0c11491>
- [93] Balbach, J. J., Ishii, Y., Antzutkin, O. N., Leapman, R. D., Rizzo, N. W., Dyda, F., et al. Amyloid fibril formation by A β 16-22, a seven-residue fragment of the Alzheimer's β -amyloid peptide, and structural characterization by solid state NMR. *Biochemistry* 39, 13748-13759 (2000). <https://doi.org/10.1021/bi0011330>
- [94] Klimov, D. K., Straub, J. E., Thirumalai, D. Aqueous urea solution destabilizes A β (16-22) oligomers. *Proc. Natl. Acad. Sci. U.S.A.* 101, 14760-14765 (2004). <https://doi.org/10.1073/pnas.0404570101>
- [95] Nguyen, P. H., Li, M. S., Derreumaux, P. Effects of all-atom force fields on amyloid oligomerization: Replica exchange molecular dynamics simulations of the A β (16-22) dimer and trimer. *Phys. Chem. Chem. Phys.* 13, 9778-9788 (2011). <https://doi.org/10.1039/c1cp20323a>
- [96] Barz, B., Wales, D. J., Strodel, B. A kinetic approach to the sequence–aggregation relationship in disease-related protein assembly. *J. Phys. Chem. B* 118, 1003-1011 (2014). <https://doi.org/10.1021/jp412648u>
- [97] Sato, S., Yoshimasa, Y., Fujita, D., Yagi-Utsumi, M., Yamaguchi, T., Kato, K., et al. A self-assembled spherical complex displaying a gangliosidic glycan cluster capable of interacting with amyloidogenic proteins. *Angew. Chem. Int. Ed.* 54, 8435-8439 (2015). <https://doi.org/10.1002/anie.201501981>
- [98] Tachi, Y., Okamoto, Y., Okumura, H. Conformational properties of an artificial GM1 glycan cluster based on a metal-ligand complex. *J. Chem. Phys.* 149, 135101 (2018). <https://doi.org/10.1063/1.5045310>
- [99] Nosé, S. A unified formulation of the constant temperature molecular dynamics methods. *J. Chem. Phys.* 81, 511-519 (1984). <https://doi.org/10.1063/1.447334>
- [100] Nosé, S. A molecular dynamics method for simulations in the canonical ensemble. *Mol. Phys.* 52, 255-268 (1984). <https://doi.org/10.1080/00268978400101201>
- [101] Hoover, W. G. Canonical dynamics: Equilibrium phase-space distributions. *Phys. Rev. A* 31, 1695-1697 (1985). <https://doi.org/10.1103/physreva.31.1695>
- [102] Andersen, H. C. Molecular dynamics simulations at constant pressure and/or temperature. *J. Chem. Phys.* 72, 2384-2393 (1980). <https://doi.org/10.1063/1.439486>
- [103] Okumura, H., Okamoto, Y. Multibaric–multithermal molecular dynamics simulation of alanine dipeptide in explicit water. *Bull. Chem. Soc. Jpn.* 80, 1114-1123 (2007). <https://doi.org/10.1246/bcsj.80.1114>
- [104] Okumura, H., Itoh, S. G., Okamoto, Y. Explicit symplectic integrators of molecular dynamics algorithms for rigid-body molecules in the canonical, isobaric-isothermal, and related ensembles. *J. Chem. Phys.* 126, 084103 (2007). <https://doi.org/10.1063/1.2434972>
- [105] Okumura, H., Okamoto, Y. Temperature and pressure dependence of alanine dipeptide studied by multibaric-multithermal molecular dynamics simulations. *J. Phys. Chem. B* 112, 12038-12049 (2008). <https://doi.org/10.1021/jp712109q>
- [106] Okumura, H. Partial multicanonical algorithm for molecular dynamics and Monte Carlo simulations. *J. Chem. Phys.* 129, 124116 (2008). <https://doi.org/10.1063/1.2970883>
- [107] Okumura, H. Optimization of partial multicanonical molecular dynamics simulations applied to an alanine dipeptide in explicit water solvent. *Phys. Chem. Chem. Phys.* 13, 114-126 (2011). <https://doi.org/10.1039/c0cp00371a>
- [108] Okumura, H. Temperature and pressure denaturation of chignolin: Folding and unfolding simulation by multibaric-multithermal molecular dynamics method. *Proteins Struct. Funct. Bioinf.* 80, 2397-2416 (2012).

- <https://doi.org/10.1002/prot.24125>
- [109] Okumura, H., Itoh, S. G. Transformation of a design peptide between the α -helix and β -hairpin structures using a helix-strand replica-exchange molecular dynamics simulation. *Phys. Chem. Chem. Phys.* 15, 13852-13861 (2013). <https://doi.org/10.1039/c3cp44443k>
- [110] Nishizawa, H., Okumura, H., Comparison of replica-permutation molecular dynamics simulations with and without detailed balance condition. *J. Phys. Soc. Jpn.* 84, 074801 (2015). <https://doi.org/10.7566/jpsj.84.074801>
- [111] Yamauchi, M., Okumura, H. Development of isothermal-isobaric replica-permutation method for molecular dynamics and Monte Carlo simulations and its application to reveal temperature and pressure dependence of folded, misfolded, and unfolded states of chignolin. *J. Chem. Phys.* 147, 184107 (2017). <https://doi.org/10.1063/1.4996431>
- [112] Yamauchi, M., Okumura, H. Replica sub-permutation method for molecular dynamics and Monte Carlo simulations. *J. Comput. Chem.* 40, 2694-2711 (2019). <https://doi.org/10.1002/jcc.26030>
- [113] Mizukami, T., Furuzawa, S., Itoh, S. G., Segawa, S., Ikura, T., Ihara, K., et al. Energetics and kinetics of substrate analog-coupled staphylococcal nuclease folding revealed by a statistical mechanical approach. *Proc. Natl. Acad. Sci. U.S.A.* 117, 19953-19962 (2020). <https://doi.org/10.1073/pnas.1914349117>
- [114] Nguyen, T. H. D., Itoh, S. G., Okumura, H., Tominaga, M. Structural basis for promiscuous action of monoterpenes on TRP channels. *Commun. Biol.* 4, 293 (2021). <https://doi.org/10.1038/s42003-021-01776-0>
- [115] Tanimoto, S., Itoh, S. G., Okumura, H. "Bucket brigade" using lysine residues in RNA-dependent RNA polymerase of SARS-CoV-2. *Biophys. J.* 120, 3615-3627 (2021). <https://doi.org/10.1016/j.bpj.2021.07.026>
- [116] Miyazawa, K., Itoh, S. G., Watanabe, H., Uchihashi, T., Yanaka, S., Yagi-Utsumi, M., et al. Tardigrade secretory-abundant heat-soluble protein has a flexible β -barrel structure in solution and keeps this structure in dehydration. *J. Phys. Chem. B* 125, 9145-9154 (2021). <https://doi.org/10.1021/acs.jpcc.1c04850>
- [117] Itoh, S. G., Tanimoto, S., Okumura, H. Dynamic properties of SARS-CoV and SARS-CoV-2 RNA-dependent RNA polymerases studied by molecular dynamics simulations. *Chem. Phys. Lett.* 778, 138819 (2021). <https://doi.org/10.1016/j.cplett.2021.138819>
- [118] Fukuhara, D., Itoh, S. G., Okumura, H. Replica permutation with solute tempering for molecular dynamics simulation and its application to the dimerization of amyloid- β fragments. *J. Chem. Phys.* 156, 084109 (2022). <https://doi.org/10.1063/5.0081686>
- [119] Mitsutake, A., Sugita, Y., Okamoto, Y. Generalized-ensemble algorithms for molecular simulations of biopolymers. *Biopolymers* 60, 96-123 (2001). [https://doi.org/10.1002/1097-0282\(2001\)60:2<96::Aid-bip1007>3.0.Co;2-f](https://doi.org/10.1002/1097-0282(2001)60:2<96::Aid-bip1007>3.0.Co;2-f)
- [120] Itoh, S. G., Okumura, H., Okamoto, Y. Generalized-ensemble algorithms for molecular dynamics simulations. *Mol. Simul.* 33, 47-56 (2007). <https://doi.org/10.1080/08927020601096812>
- [121] Okumura, H., Itoh, S. G., Okamoto, Y. Generalized-ensemble algorithms for simulations of complex molecular systems. in *Practical Aspects of Computational Chemistry II: An Overview of the Last Two Decades and Current Trends* (Leszczynski, J., Shukla M.K. eds.) pp. 69-101 (Springer Netherlands, Dordrecht, 2012).
- [122] Yamauchi, M., Mori, Y., Okumura, H. Molecular simulations by generalized-ensemble algorithms in isothermal-isobaric ensemble. *Biophys. Rev.* 11, 457-469 (2019). <https://doi.org/10.1007/s12551-019-00537-y>
- [123] Itoh, S. G., Okumura, H. All-atom molecular dynamics simulation methods for the aggregation of protein and peptides: Replica exchange/permutation and nonequilibrium simulations. in *Computer Simulations of Aggregation of Proteins and Peptides* (Li, M. S., Kloczkowski, A., Cieplak, M., Kouza M. eds.) pp. 197-220 (Humana, New York, NY, 2022).
- [124] Hukushima, K., Nemoto, K. Exchange Monte Carlo method and application to spin glass simulations. *J. Phys. Soc. Jpn.* 65, 1604-1608 (1996). <https://doi.org/10.1143/JPSJ.65.1604>
- [125] Sugita, Y., Okamoto, Y. Replica-exchange molecular dynamics method for protein folding. *Chem. Phys. Lett.* 314, 141-151 (1999). [https://doi.org/10.1016/S0009-2614\(99\)01123-9](https://doi.org/10.1016/S0009-2614(99)01123-9)
- [126] Itoh, S. G., Okumura, H. Replica-permutation method with the Suwa-Todo algorithm beyond the replica-exchange method. *J. Chem. Theory Comput.* 9, 570-581 (2013). <https://doi.org/10.1021/ct3007919>
- [127] Berg, B. A., Neuhaus, T. Multicanonical algorithms for 1st order phase-transitions. *Phys. Lett. B* 267, 249-253 (1991). [https://doi.org/10.1016/0370-2693\(91\)91256-u](https://doi.org/10.1016/0370-2693(91)91256-u)
- [128] Berg, B. A., Neuhaus, T. Multicanonical ensemble: A new approach to simulate first-order phase transitions. *Phys. Rev. Lett.* 68, 9-12 (1992). <https://doi.org/10.1103/PhysRevLett.68.9>
- [129] Hansmann, U. H. E., Okamoto, Y., Eisenmenger, F. Molecular dynamics, Langevin and hybrid Monte Carlo simulations in a multicanonical ensemble. *Chem. Phys. Lett.* 259, 321-330 (1996). [https://doi.org/10.1016/0009-2614\(96\)00761-0](https://doi.org/10.1016/0009-2614(96)00761-0)
- [130] Nakajima, N., Nakamura, H., Kidera, A. Multicanonical ensemble generated by molecular dynamics simulation for enhanced conformational sampling of peptides. *J. Phys. Chem. B* 101, 817-824 (1997).

- <https://doi.org/10.1021/jp962142e>
- [131] Okumura, H., Okamoto, Y. Monte Carlo simulations in multibaric–multithermal ensemble. *Chem. Phys. Lett.* 383, 391-396 (2004). <https://doi.org/10.1016/j.cplett.2003.10.152>
- [132] Okumura, H., Okamoto, Y. Monte Carlo simulations in generalized isobaric-isothermal ensembles. *Phys. Rev. E* 70, 026702 (2004). <https://doi.org/10.1103/PhysRevE.70.026702>
- [133] Okumura, H., Okamoto, Y. Molecular dynamics simulations in the multibaric–multithermal ensemble. *Chem. Phys. Lett.* 391, 248-253 (2004). <https://doi.org/10.1016/j.cplett.2004.04.073>
- [134] Okumura, H., Okamoto, Y. Multibaric-multithermal ensemble molecular dynamics simulations. *J. Comput. Chem.* 27, 379-395 (2006). <https://doi.org/10.1002/jcc.20351>
- [135] Utsumi, M., Yamaguchi, Y., Sasakawa, H., Yamamoto, N., Yanagisawa, K., Kato, K. Up-and-down topological mode of amyloid β -peptide lying on hydrophilic/hydrophobic interface of ganglioside clusters. *Glycoconj. J.* 26, 999-1006 (2009). <https://doi.org/10.1007/s10719-008-9216-7>
- [136] Yagi-Utsumi, M., Matsuo, K., Yanagisawa, K., Gekko, K., Kato, K. Spectroscopic characterization of intermolecular interaction of amyloid β promoted on GM1 micelles. *Int. J. Alzheimers Dis.* 2011, 925073 (2010). <https://doi.org/10.4061/2011/925073>
- [137] Buch, V., Milet, A., Vacha, R., Jungwirth, P., Devlin, J. P. Water surface is acidic. *Proc. Natl. Acad. Sci. U.S.A.* 104, 7342-7347 (2007). <https://doi.org/10.1073/pnas.0611285104>
- [138] Beattie, J. K., Djerdjev, A. M., Warr, G. G. The surface of neat water is basic. *Faraday Discuss.* 141, 31-39; discussion 81-98 (2009). <https://doi.org/10.1039/b805266b>
- [139] Wei, H., Vejerano, E. P., Leng, W., Huang, Q., Willner, M. R., Marr, L. C., et al. Aerosol microdroplets exhibit a stable pH gradient. *Proc. Natl. Acad. Sci. U.S.A.* 115, 7272-7277 (2018). <https://doi.org/10.1073/pnas.1720488115>
- [140] Sen, P., Yamaguchi, S., Tahara, T. New insight into the surface denaturation of proteins: Electronic sum frequency generation study of cytochrome c at water interfaces. *J. Phys. Chem. B* 112, 13473-13475 (2008). <https://doi.org/10.1021/jp8061288>
- [141] Abelein, A., Abrahams, J. P., Danielsson, J., Gräslund, A., Jarvet, J., Luo, J., et al. The hairpin conformation of the amyloid- β peptide is an important structural motif along the aggregation pathway. *J. Biol. Inorg. Chem.* 19, 623-634 (2014). <https://doi.org/10.1007/s00775-014-1131-8>
- [142] Maity, S., Hashemi, M., Lyubchenko, Y. L. Nano-assembly of amyloid β peptide: role of the hairpin fold. *Sci. Rep.* 7, 2344 (2017). <https://doi.org/10.1038/s41598-017-02454-0>
- [143] Schneider, T., Stoll, E. Molecular-dynamics study of a three-dimensional one-component model for distortive phase transitions. *Phys. Rev. B* 17, 1302-1322 (1978). <https://doi.org/10.1103/PhysRevB.17.1302>
- [144] Berendsen, H. J. C., Postma, J. P. M., Gunsteren, W. F. v., DiNola, A., Haak, J. R. Molecular dynamics with coupling to an external bath. *J. Chem. Phys.* 81, 3684-3690 (1984). <https://doi.org/10.1063/1.448118>
- [145] Ikeda, K., Yamaguchi, T., Fukunaga, S., Hoshino, M., Matsuzaki, K. Mechanism of amyloid β -protein aggregation mediated by GM1 ganglioside clusters. *Biochemistry* 50, 6433-6440 (2011). <https://doi.org/10.1021/bi200771m>

